

Band gaps of wurtzite $\text{Sc}_x\text{Ga}_{1-x}\text{N}$ alloys

H. C. L. Tsui, L. E. Goff, S. K. Rhode, S. Pereira, H. E. Beere, I. Farrer, C. A. Nicoll, D. A. Ritchie, and M. A. Moram

Citation: *Appl. Phys. Lett.* **106**, 132103 (2015); doi: 10.1063/1.4916679

View online: <http://dx.doi.org/10.1063/1.4916679>

View Table of Contents: <http://aip.scitation.org/toc/apl/106/13>

Published by the [American Institute of Physics](http://www.aip.org)



**THE WORLD'S RESOURCE FOR
VARIABLE TEMPERATURE
SOLID STATE CHARACTERIZATION**



OPTICAL STUDIES SYSTEMS



SEEBECK STUDIES SYSTEMS



MICROPROBE STATIONS



HALL EFFECT STUDY SYSTEMS AND MAGNETS

WWW.MMR-TECH.COM

Band gaps of wurtzite $\text{Sc}_x\text{Ga}_{1-x}\text{N}$ alloys

H. C. L. Tsui,¹ L. E. Goff,^{1,2} S. K. Rhode,³ S. Pereira,⁴ H. E. Beere,² I. Farrer,² C. A. Nicoll,² D. A. Ritchie,² and M. A. Moram¹

¹Department of Materials, Imperial College London, Exhibition Road, London SW7 2AZ, United Kingdom

²Department of Physics, University of Cambridge, JJ Thomson Avenue, Cambridge CB3 0HE, United Kingdom

³Department of Materials Science and Metallurgy, University of Cambridge, Charles Babbage Road, Cambridge CB3 0FS, United Kingdom

⁴CICECO and Dept. Physics, Universidade de Aveiro, 3810 193 Aveiro, Portugal

(Received 2 February 2015; accepted 17 March 2015; published online 30 March 2015)

Optical transmittance measurements on epitaxial, phase-pure, wurtzite-structure $\text{Sc}_x\text{Ga}_{1-x}\text{N}$ films with $0 \leq x \leq 0.26$ showed that their direct optical band gaps increased from 3.33 eV to 3.89 eV with increasing x , in agreement with theory. These films contained I_1 - and I_2 -type stacking faults. However, the direct optical band gaps decreased from 3.37 eV to 3.26 eV for $\text{Sc}_x\text{Ga}_{1-x}\text{N}$ films, which additionally contained nanoscale lamellar inclusions of the zinc-blende phase, as revealed by aberration-corrected scanning transmission electron microscopy. Therefore, we conclude that the apparent reduction in $\text{Sc}_x\text{Ga}_{1-x}\text{N}$ band gaps with increasing x is an artefact resulting from the presence of nanoscale zinc-blende inclusions. © 2015 AIP Publishing LLC.

[<http://dx.doi.org/10.1063/1.4916679>]

The wurtzite-structure III-nitrides AlN, GaN, and InN are widely used in optoelectronic and high-power electronic applications, including high mobility electron transistors, energy harvesters, laser diodes, and light emitting diodes (LEDs). Alloying nitride semiconductors enable band gap engineering, which allows the range of emission wavelengths in optoelectronic devices to be tuned, e.g., within the ultraviolet (UV) and green emission regions for $\text{Al}_x\text{Ga}_{1-x}\text{N}$ (Ref. 1) and $\text{In}_x\text{Ga}_{1-x}\text{N}$,² respectively. However, devices made using these materials can suffer from poor efficiencies, especially in the UV region. This is attributed to difficulties in p -type doping these wide band gap materials, along with lattice parameter mismatches between different layers in the epitaxial devices, leading to the build-up of in-plane stress, film cracking, and high dislocation densities.³ These problems are related to the fundamental electronic structure of $\text{Al}_x\text{Ga}_{1-x}\text{N}$ semiconductors and to the relationship between their band gaps and lattice parameters. Consequently, there is considerable motivation to find alternative wide band gap semiconductors for use in UV optoelectronics, which have different electronic structures and different relationships between their lattice parameters and direct band gaps. Alloying GaN with ScN offers interesting possibilities in this regard.⁴

ScN is a rock-salt structure semiconductor with a direct band gap of 2.1 eV and an indirect band gap of 0.9 eV,⁵⁻⁷ which can be grown easily by molecular beam epitaxy (MBE)⁸ and which has already been used in as a dislocation reduction interlayer in GaN films⁹ and is of interest for thermoelectric applications.^{8,10,11} The phase stability, structural, and optical properties of ScN and $\text{Sc}_x\text{Ga}_{1-x}\text{N}$ have been calculated previously. Farrer and Bellaiche predicted that the ScN is unstable in the wurtzite structure but metastable in an h -BN-like non-polar structure.¹² All studies have predicted that $\text{Sc}_x\text{Ga}_{1-x}\text{N}$ alloys will be metastable with respect to rock-salt structure ScN and wurtzite-structure GaN. However, in

practice, $\text{Sc}_x\text{Ga}_{1-x}\text{N}$ alloys can be grown in epitaxial thin film form under a range of growth conditions.¹³⁻¹⁵ Recent high-quality calculations also concluded that (0001)-oriented $\text{Sc}_x\text{Ga}_{1-x}\text{N}$ films can be stabilised using in-plane compressive epitaxial strain (e.g., by growing on top of GaN layers) and/or by using non-equilibrium growth conditions. In that case, $\text{Sc}_x\text{Ga}_{1-x}\text{N}$ alloys are expected to retain the wurtzite structure up to an intermediate Sc content of around $x=0.66$.¹⁶ However, there is controversy over the band gaps of $\text{Sc}_x\text{Ga}_{1-x}\text{N}$ alloys in the literature. Constantin *et al.* predicted that the band gaps of $\text{Sc}_x\text{Ga}_{1-x}\text{N}$ should decrease as the Sc content increases,¹³ however, their calculations assumed that the alloys retained an undistorted wurtzite structure throughout, which does not match lattice parameter data obtained from experiment¹⁷ or from later theoretical calculations.¹⁶ Farrer and Bellaiche also predicted that the band gap of $\text{Sc}_x\text{Ga}_{1-x}\text{N}$ should decrease from 3.5 eV (the band gap of GaN) to 1.55 eV (the band gap of h -BN-like ScN) as the Sc concentration increases.¹² On the other hand, Zhang *et al.* predicted that the direct band gaps should increase from 3.5 eV (GaN) to 4.36 eV ($\text{Sc}_{0.5}\text{Ga}_{0.5}\text{N}$) as the Sc content increases, and will then decrease to 1.5 eV as the Sc content increases further and a phase change to the cubic structure occurs. Experimental results from Little and Kordesch¹⁸ and Constantin *et al.*¹⁷ showed a decrease in the magnitude of the direct optical band gap as the Sc content increased, however, the films possessed either poor crystal quality¹⁸ and/or an extremely high density of stacking faults.¹⁷ Epitaxial (0001)-oriented wurtzite-structure $\text{Sc}_x\text{Ga}_{1-x}\text{N}$ films can also contain cubic inclusions (i.e., lamellae with the zinc-blende structure oriented along the (0001) plane¹⁹), which are difficult to distinguish from stacking faults in high-resolution transmission electron microscopy (TEM) images. All of these may lead to sub-gap absorption and misleading conclusions about the trend in band gaps as a function of the Sc content. Therefore, this study aims to understand the influence of film

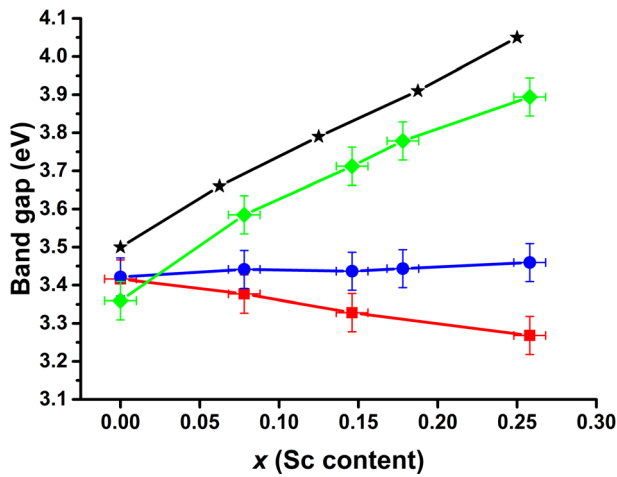


FIG. 1. Band gaps of $\text{Sc}_x\text{Ga}_{1-x}\text{N}$ with $0 \leq x \leq 0.26$, grown on different buffer layers. Red square: $\text{Sc}_x\text{Ga}_{1-x}\text{N}$ on MBE GaN; Blue circle: $\text{Sc}_x\text{Ga}_{1-x}\text{N}$ on MOVPE GaN; Green diamond: $\text{Sc}_x\text{Ga}_{1-x}\text{N}$ on MOVPE AlN; Black star: calculation results adapted from Ref. 16.

microstructure on the direct optical band gaps of epitaxial $\text{Sc}_x\text{Ga}_{1-x}\text{N}$ films, and thereby to determine which of the predicted trends in band gap versus composition is correct.

Epitaxial wurtzite-structure (0001)-oriented $\text{Sc}_x\text{Ga}_{1-x}\text{N}$ films were grown using MBE with an N_2 plasma source, under metal-rich growth conditions. Three different kinds of buffer layers were used to influence the $\text{Sc}_x\text{Ga}_{1-x}\text{N}$ film strain state and microstructure: (0001)-oriented GaN grown by molecular beam epitaxy on sapphire, (0001)-oriented GaN grown by metal-organic vapour phase epitaxy (MOVPE), and (0001)-oriented AlN grown by metal-organic vapour phase epitaxy. The $\text{Sc}_x\text{Ga}_{1-x}\text{N}$ film compositions were controlled by varying the Sc flux while keeping the Ga flux constant and the N_2 flow rate constant values, which produce a GaN growth rate of approximately 260 nm h^{-1} . Film compositions were determined using Rutherford backscattering (RBS). RBS measurements were performed using a beam of ^4He at 2 MeV with an incidence angle of 0° . A standard detector was placed at 140° and two pin-diode detectors located symmetrically to each other at 165° . The RBS data were analysed using the IBA DataFurnace NDF v9.6d.²⁰ Optical transmittance measurements were carried out using an Agilent Technologies Cary 5000 UV-Vis-NIR spectrophotometer at room temperature, using a bare sapphire substrate as a reference. To minimise the unintentional incorporation of impurities, the MBE chamber was operated at a low base pressure of 10^{-10} mbar, and the scandium metal was custom-prepared for high purity (Sc 99.999%) and no detectable fluorine.

TEM analysis was carried out using a JEOL 2100 at 200 kV. Cross-sectional TEM samples were prepared by mechanical grinding followed by ion polishing until electron transparency was reached. Aberration-corrected high angle annular dark field (HAADF) imaging in the scanning TEM (STEM) mode was performed on the Titan³ 80 300 at 300 kV with a probe convergence semi-angle of 15 mrad. Spherical aberrations up to the third order in the electron beam “probe” were corrected by recording Zemlin tableau diffractograms.

Figure 1 shows the direct optical band gaps of $\text{Sc}_x\text{Ga}_{1-x}\text{N}$ grown on different buffer layers. For $\text{Sc}_x\text{Ga}_{1-x}\text{N}$ grown on MBE GaN buffer layers, the band gap decreased as the Sc content increased. The same trend was found previously by Little and Kordesch¹⁸ and Constantin *et al.*¹⁷ for the $\text{Sc}_x\text{Ga}_{1-x}\text{N}$ films with the poor crystal quality or high densities of stacking faults. In contrast, measurements from the $\text{Sc}_x\text{Ga}_{1-x}\text{N}$ films on MOVPE GaN are limited by the lower band gap of the GaN buffer layer (3.4 eV at room temperature²¹), indicating that the band gaps of the $\text{Sc}_x\text{Ga}_{1-x}\text{N}$ films are higher than GaN. However, AlN has a very wide band gap of 6.2 eV at room temperature, so the band gaps of $\text{Sc}_x\text{Ga}_{1-x}\text{N}$ can be revealed in optical absorption measurements. Figure 1 shows clearly that the band gaps of the $\text{Sc}_x\text{Ga}_{1-x}\text{N}$ films grown on AlN increase with increasing the Sc content, in agreement with recent high-quality theoretical predictions.¹⁶ However, the measured band gaps of $\text{Sc}_x\text{Ga}_{1-x}\text{N}$ are approximately 0.1 eV lower than the predicted values. This arises because in the previous theoretical study, the predicted band gap of GaN was corrected to 3.5 eV, i.e., the value it takes a temperature close to 0 K, which is appropriate for comparison to the calculated data.²² In contrast, if the theoretical data are corrected with respect to the room-temperature band gap of GaN of 3.4 eV,²¹ then the theoretical and experimental data match very well. Importantly, reference samples of ScN and GaN prepared in the same MBE reactor under comparable conditions had band gaps of 2.1 eV and 3.4 eV, respectively, which are the literature values for pure films. This indicates minimal oxygen contamination and suggests that the films are stoichiometric, as impurities and vacancies are known to affect the band gap of ScN.^{23,24}

Microstructural analysis was performed to understand the effect of defects on the band gaps of $\text{Sc}_x\text{Ga}_{1-x}\text{N}$. I_1 - and I_2 -type basal-plane stacking faults (BSFs) were seen in all the $\text{Sc}_x\text{Ga}_{1-x}\text{N}$ films (Figure 2). This suggests that the stacking faults are not responsible for the lower band gaps measured in $\text{Sc}_x\text{Ga}_{1-x}\text{N}$ on MBE GaN. On the other hand, aberration-corrected STEM-HAADF images acquired along the $\langle 11\bar{2}0 \rangle$ zone axis showed cubic stacking (ABCABC)

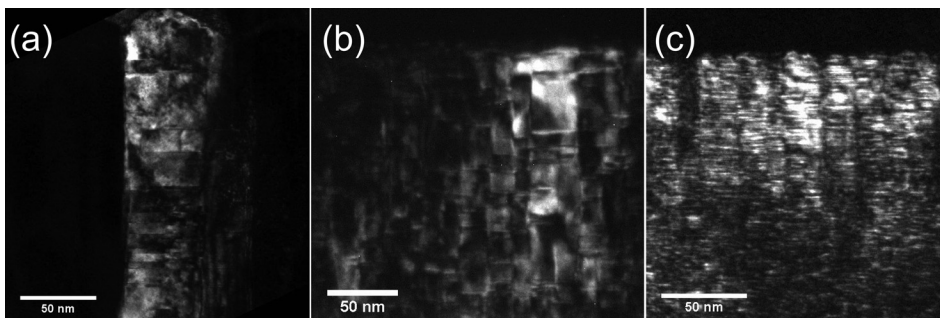


FIG. 2. Dark field TEM images acquired along the $\langle 11\bar{2}0 \rangle$ zone axis of $\text{Sc}_x\text{Ga}_{1-x}\text{N}$ on different buffer layers, (a) MBE GaN, (b) MOVPE GaN, and (c) MOVPE AlN.

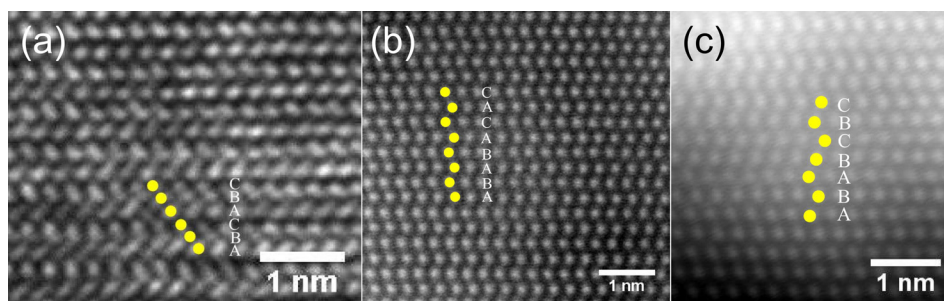


FIG. 3. (a) Cubic stacking, found only in $\text{Sc}_x\text{Ga}_{1-x}\text{N}$ on MBE GaN, (b) I_1 and (c) I_2 basal plane stacking faults found in all samples using aberration corrected STEM with specimens oriented along the $\langle 11\bar{2}0 \rangle$ zone axis.

only in $\text{Sc}_x\text{Ga}_{1-x}\text{N}$ on MBE GaN (Figure 3), which has been observed previously in $\text{Sc}_x\text{Ga}_{1-x}\text{N}$ grown by NH_3 -MBE and which can be distinguished from the expected rock-salt phase.¹⁹ No significant differences in contrast to the STEM images can be seen between the regions with cubic stacking (these are effectively one large stacking fault) and the rest of the material, indicating minimal compositional differences. However, the zinc blende phase of GaN has a band gap approximately 0.2 eV lower than that of hexagonal GaN,^{25,26} and the band gap of zinc-blende ScN is expected to be lower than that of zinc-blende GaN,²⁷ such that the band gap of the inclusions should decrease with increasing the Sc content. Therefore, we conclude that the inclusions of the zinc blende phase are the cause of the apparent reduction in band gap with increasing the Sc content. Importantly, it is very difficult to distinguish nanoscale lamellar inclusions layered along (0001) from BSFs using high-resolution TEM imaging, as used in Ref. 13: hence, zinc blende inclusions could have been present in those samples too and could account for the apparent decrease in band gap of $\text{Sc}_x\text{Ga}_{1-x}\text{N}$ with increasing the Sc content, as reported in the previous work.

In conclusion, the band gaps of $\text{Sc}_x\text{Ga}_{1-x}\text{N}$ films were found to increase with increasing the Sc content for $\text{Sc}_x\text{Ga}_{1-x}\text{N}$ grown on MOVPE GaN and AlN buffer layers, in agreement with recent high-quality calculations.¹⁶ In contrast, band gaps of $\text{Sc}_x\text{Ga}_{1-x}\text{N}$ grown on MBE GaN decrease with increasing the Sc content, consistent with previous experimental reports. Although, I_1 - and I_2 -type basal-plane stacking faults were seen in all $\text{Sc}_x\text{Ga}_{1-x}\text{N}$ films, lamellar inclusions of the cubic phase were found only in $\text{Sc}_x\text{Ga}_{1-x}\text{N}$ on MBE GaN, and are believed to produce sub-gap optical absorption. Therefore, $\text{Sc}_x\text{Ga}_{1-x}\text{N}$ films may prove useful in UV optoelectronic applications, as long as the buffer layers and growth conditions are selected to minimise the formation of cubic inclusions.

M.A.M. acknowledges support through a Royal Society University Research Fellowship and through ERC Starting Grant “SCOPE.” The authors also acknowledge microscope facility time from Professor C. J. Humphreys.

- ¹A. Khan, K. Balakrishnan, and T. Katona, *Nat. Photonics* **2**, 77 (2008).
- ²T. Mukai, M. Yamada, and S. Nakamura, *Jpn. J. Appl. Phys., Part 1* **38**, 3976 (1999).
- ³M. Kneissl, T. Kolbe, C. Chua, V. Kueller, N. Lobo, J. Stellmach, A. Knauer, H. Rodriguez, S. Einfeldt, Z. Yang, N. M. Johnson, and M. Weyers, *Semicond. Sci. Technol.* **26**, 014036 (2011).
- ⁴M. A. Moram and S. Zhang, *J. Mater. Chem. A* **2**, 6042 (2014).
- ⁵W. R. L. Lambrecht, *Phys. Rev. B* **62**, 13538 (2000).
- ⁶A. R. Smith, H. A. H. Al Brithen, D. C. Ingram, and D. Gall, *J. Appl. Phys.* **90**, 1809 (2001).
- ⁷D. Gall, I. Petrov, L. D. Madsen, J. E. Sundgren, and J. E. Greene, *J. Vac. Sci. Technol., A* **16**, 2411 (1998).
- ⁸S. Kerdsonpanya, N. V. Nong, N. Pryds, A. Zukauskaitė, J. Jensen, J. Birch, J. Lu, L. Hultman, G. Wingqvist, and P. Eklund, *Appl. Phys. Lett.* **99**, 232113 (2011).
- ⁹M. A. Moram, Y. Zhang, M. J. Kappers, Z. H. Barber, and C. J. Humphreys, *Appl. Phys. Lett.* **91**, 152101 (2007).
- ¹⁰H. A. Al Brithen, A. R. Smith, and D. Gall, *Phys. Rev. B* **70**, 045303 (2004).
- ¹¹P. V. Burmistrova, J. Maassen, T. Favalaro, B. Saha, S. Salamat, Y. R. Koh, M. S. Lundstrom, A. Shakouri, and T. D. Sands, *J. Appl. Phys.* **113**, 153704 (2013).
- ¹²N. Farrer and L. Bellaiche, *Phys. Rev. B* **66**, 201203 (2002).
- ¹³C. Constantin, M. B. Haider, D. Ingram, A. R. Smith, N. Sandler, K. Sun, and P. Ordejon, *J. Appl. Phys.* **98**, 123501 (2005).
- ¹⁴M. A. Moram, Y. Zhang, T. B. Joyce, D. Holec, P. R. Chalker, P. H. Mayrhofer, M. J. Kappers, and C. J. Humphreys, *J. Appl. Phys.* **106**, 113533 (2009).
- ¹⁵S. M. Knoll, S. Zhang, T. B. Joyce, M. J. Kappers, C. J. Humphreys, and M. A. Moram, *Phys. Status Solidi A* **209**, 33 (2012).
- ¹⁶S. Zhang, D. Holec, W. Y. Fu, C. J. Humphreys, and M. A. Moram, *J. Appl. Phys.* **114**, 133510 (2013).
- ¹⁷C. Constantin, H. Al Brithen, M. B. Haider, D. Ingram, and A. R. Smith, *Phys. Rev. B* **70**, 193309 (2004).
- ¹⁸M. E. Little and M. E. Kordes, *Appl. Phys. Lett.* **78**, 2891 (2001).
- ¹⁹S. M. Knoll, S. K. Rhode, S. Zhang, T. B. Joyce, and M. A. Moram, *Appl. Phys. Lett.* **104**, 101906 (2014).
- ²⁰N. P. Barradas, E. Alves, C. Jeyes, and M. Tosaki, *Nucl. Instrum. Methods Phys. Res., Sect. B* **247**, 381 (2006).
- ²¹S. Strite and H. Morkoc, *J. Vac. Sci. Technol., B* **10**, 1237 (1992).
- ²²R. Dingle, D. D. Sell, S. E. Stokowski, and M. Ilegems, *Phys. Rev. B* **4**, 1211 (1971).
- ²³S. Kerdsonpanya, B. Alling, and P. Eklund, *Phys. Rev. B* **86**, 195140 (2012).
- ²⁴M. A. Moram, Z. H. Barber, and C. J. Humphreys, *Thin Solid Films* **516**, 8569 (2008).
- ²⁵H. Okumura, K. Ohta, K. Ando, W. W. Ruhle, T. Nagatomo, and S. Yoshida, *Solid State Electron.* **41**, 201 (1997).
- ²⁶A. Philippe, C. Bru Chevallier, M. Vernay, G. Guillot, J. Hubner, B. Daudin, and G. Feuillet, *Mater. Sci. Eng., B* **59**, 168 (1999).
- ²⁷A. Tebboune, D. Rached, A. Benzair, N. Sekkal, and A. Belbachir, *Phys. Status Solidi B* **243**, 2788 (2006).